

Time-resolved structural studies with serial crystallography: A new light on retinal proteins

Valérie Panneels, Wenting Wu, Ching-Ju Tsai, Przemek Nogly, Jan Rheinberger, Kathrin Jaeger, Gregor Cicchetti, Cornelius Gati, Leonhard M. Kick, Leonardo Sala, Guido Capitani, Chris Milne, Celestino Padeste, Bill Pedrini, Xiao-Dan Li, Jörg Standfuss, Rafael Abela, and Gebhard Schertler

Citation: *Structural Dynamics* **2**, 041718 (2015); doi: 10.1063/1.4922774

View online: <http://dx.doi.org/10.1063/1.4922774>

View Table of Contents: <http://scitation.aip.org/content/aca/journal/sdy/2/4?ver=pdfcov>

Published by the [American Crystallographic Association, Inc.](#)

Articles you may be interested in

[Possibilities for serial femtosecond crystallography sample delivery at future light sources](#)

Struct. Dyn. **2**, 041709 (2015); 10.1063/1.4921220

[A split-beam probe-pump-probe scheme for femtosecond time resolved protein X-ray crystallography](#)

Struct. Dyn. **2**, 014102 (2015); 10.1063/1.4906354

[Steady state, time resolved, and circular dichroism spectroscopic studies to reveal the nature of interactions of zinc oxide nanoparticles with transport protein bovine serum albumin and to monitor the possible protein conformational changes](#)

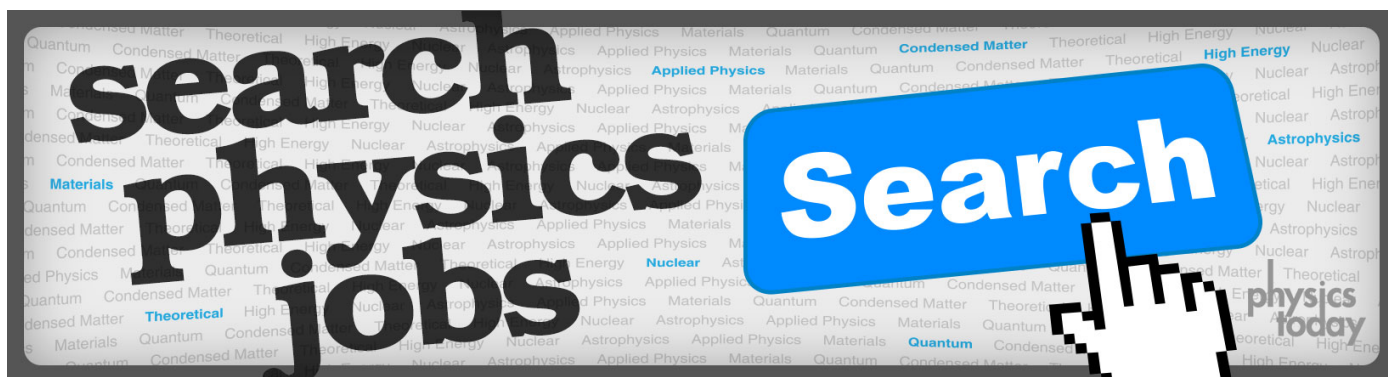
J. Appl. Phys. **106**, 034701 (2009); 10.1063/1.3190483

[Neutron Protein Crystallography: Beyond the Folding Structure](#)

AIP Conf. Proc. **989**, 47 (2008); 10.1063/1.2906091

[Spectral diffusion in glasses under high pressure: A study by time-resolved hole-burning](#)

J. Chem. Phys. **110**, 7467 (1999); 10.1063/1.478649



Time-resolved structural studies with serial crystallography: A new light on retinal proteins

Valérie Panneels,¹ Wenting Wu,¹ Ching-Ju Tsai,¹ Przemek Nogly,¹
Jan Rheinberger,¹ Kathrin Jaeger,¹ Gregor Cicchetti,¹ Cornelius Gati,^{1,2}
Leonhard M. Kick,¹ Leonardo Sala,³ Guido Capitani,¹ Chris Milne,⁴
Celestino Padeste,⁵ Bill Pedrini,⁴ Xiao-Dan Li,¹ Jörg Standfuss,¹
Rafael Abela,⁴ and Gebhard Schertler^{1,6}

¹Laboratory of Biomolecular Research, Paul Scherrer Institute, 5232 Villigen PSI, Switzerland

²Center for Free-Electron Laser Science (CFEL), Deutsches Elektronensynchrotron (DESY), Notkestrasse 85, 22607 Hamburg, Germany

³Scientific Computing, Paul Scherrer Institute, 5232 Villigen PSI, Switzerland

⁴SwissFEL Paul Scherrer Institute, 5232 Villigen PSI, Switzerland

⁵Lab for Micro- and Nanotechnology, Paul Scherrer Institute, 5232 Villigen PSI, Switzerland

⁶Department of Biology, ETH Zurich, Zurich, Switzerland

(Received 31 March 2015; accepted 3 June 2015; published online 29 June 2015)

Structural information of the different conformational states of the two prototypical light-sensitive membrane proteins, bacteriorhodopsin and rhodopsin, has been obtained in the past by X-ray cryo-crystallography and cryo-electron microscopy. However, these methods do not allow for the structure determination of most intermediate conformations. Recently, the potential of X-Ray Free Electron Lasers (X-FELs) for tracking the dynamics of light-triggered processes by pump-probe serial femtosecond crystallography has been demonstrated using 3D-micron-sized crystals. In addition, X-FELs provide new opportunities for protein 2D-crystal diffraction, which would allow to observe the course of conformational changes of membrane proteins in a close-to-physiological lipid bilayer environment. Here, we describe the strategies towards structural dynamic studies of retinal proteins at room temperature, using injector or fixed-target based serial femtosecond crystallography at X-FELs. Thanks to recent progress especially in sample delivery methods, serial crystallography is now also feasible at synchrotron X-ray sources, thus expanding the possibilities for time-resolved structure determination. © 2015 Author(s). All article content, except where otherwise noted, is licensed under a Creative Commons Attribution 3.0 Unported License. [<http://dx.doi.org/10.1063/1.4922774>]

INTRODUCTION

The function of a protein is determined by its structure which defines specific properties in a biological context and its dynamic interactions with diverse partners such as ions, lipids, hormones, other proteins, and nucleic acids. Detailed structural information on protein complexes has had tremendous impact on our understanding of biological systems and is critical for rational drug discovery, rationally designed protein engineering, and biocatalysis. However, static structural information also has its limitations since the biological function of most proteins is dependent on conformational changes in response to stimuli or protein-protein interactions. Dynamic information of protein motions covering their conformational landscape together with structural information would therefore lead to a more precise understanding of their biological role and drastically improve our ability for rational protein engineering.



SERIAL FEMTOSECOND CRYSTALLOGRAPHY (SFX)

About 90% of all structures in the Protein Data Bank have been obtained by X-ray crystallography. This method relies on crystals to amplify the structural information and reach sufficient signal to noise ratios. Unfortunately, this method delivers the best results with large, well-ordered crystals that are often difficult to obtain, especially for membrane proteins. Radiation damage poses another fundamental barrier that limits the achievable data quality and may alter the structure of proteins in possibly misleading ways.

X-ray free electron lasers (X-FELs) overcome limitations of classical crystallography by outrunning radiation damage with highly brilliant femtosecond X-ray pulses briefer than the timescale of most crystal damage processes (Neutze *et al.*, 2000). The high brilliance of the X-ray pulses also allows for collecting data from crystals smaller than few micrometers, which is impossible at synchrotron sources. As individual crystals are destroyed immediately after data collection, a stream of new crystals is injected into the X-ray path for each X-FEL pulse to ensure continuous data collection. The achieved resolution in the first SFX experiments was constrained by experimental conditions, namely, a photon energy of 2 keV, but the obtained dataset was sufficient to produce an 8.5 Å resolution electron density map (Chapman *et al.*, 2011). Since this initial demonstration, a number of major breakthroughs have been achieved, including a 1.9 Å resolution structure of lysozyme as the first high-resolution structure from SFX (Boutet *et al.*, 2012).

DEVELOPMENT OF NOVEL SAMPLE DELIVERY MODES

X-FEL technology requires the development of new delivery strategies due to the high X-ray intensities used in the “diffract before destroy” regime of SFX (Neutze *et al.*, 2000). The crystals are sequentially passing into the X-ray beam either by flowing in a mobile phase using a microjet (Fig. 1(b)) or by being scanned on a solid support (Fig. 1(a)). In time-resolved SFX (TR-SFX) experiments, liquid jets such as the most commonly used gas dynamic virtual nozzle (GDVN) (Weierstall *et al.*, 2012) allow for crystals being constantly replenished, thus preventing multiple laser excitations of the same crystal. However, this requires milliliters of a crystal suspension (the flow rate of the GDVN liquid jet is at least $10 \mu\text{l min}^{-1}$), which is a major hurdle for the general application of liquid jet-based SFX. This has triggered the development of

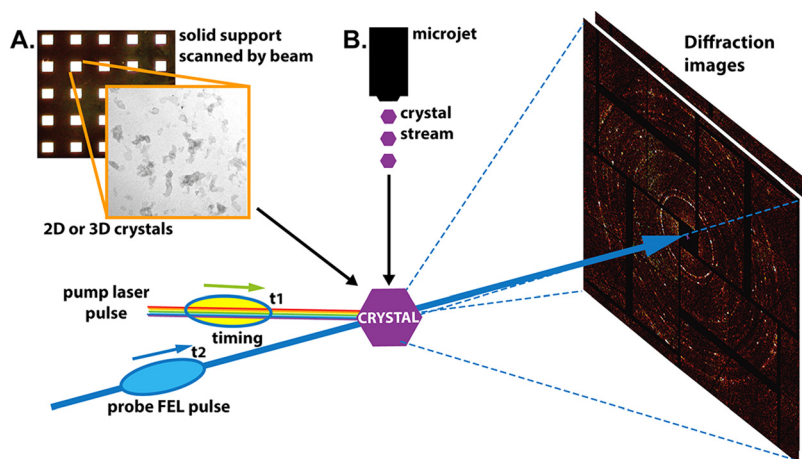


FIG. 1. Scheme of pump-probe time-resolved SFX experimental setup for retinal protein dynamics study. The figure shows the overall setup containing the optical pump laser (rainbow), the probe X-ray FEL pulse (in blue), and the detectors. The high X-FEL intensities used in the “diffract before destroy” regime of SFX require a constant delivery of crystals at room temperature, precisely aligned with the path of the pump laser which is set at the wavelength specific for the retinal protein photoactivation. After a precise time-delay, the X-FEL pulse is delivered in the interaction region to record the structural information about the induced changes. To date, among the various sample delivery modes available for SFX, including fixed target wafers (a) with arrays of windows with painted 2D or 3D crystals in a glucose-containing solution, only the microjet (b) system delivering a liquid stream of submicron crystals is used for TR-SFX.

the electrospinning liquid microjet (Sierra *et al.*, 2012), the microfluidics drop-on-demand jet (Perry *et al.*, 2014), as well as the lipidic cubic phase (LCP) injector system. The LCP injector, in particular, is ideal for membrane proteins and reduces sample consumption at least 100 fold (Weierstall *et al.*, 2014). With LCP jets now being available, the rate of structure determination of important membrane protein targets is quickly growing (Liu *et al.*, 2013 and Weierstall *et al.*, 2014). A recent adaptation of this technology for usage at the more widely available synchrotron microfocus beamlines (Nogly *et al.*, 2015) and the introduction of slow-flowing, high-viscosity matrices compatible with delivery of soluble proteins (Sugahara *et al.*, 2015 and Botha *et al.*, 2015) dramatically increase the range of applications for serial crystallography. Using such injector systems, routine collection of diffraction patterns from fully hydrated samples in a native-like lipidic environment, at room temperature, and with negligible radiation damage becomes a real possibility.

Beside the jet type of delivery, fixed targets covered by crystals have shown to be particularly useful for some applications. The crystals are typically supported by a solid silicon wafer, shaped with an extended array of $100 \times 100 \mu\text{m}^2$ windows consisting of 20–30 nm thick silicon nitride. Alternatively, a 5 nm carbon film with a 40 nm poly-(methyl methacrylate) layer was used as the window material. The crystals suspended in a glucose solution were painted on the backside of the wafer, so that they could adhere to the carbon face of the windows. After drying, the remaining layer of glucose acts as protection against dehydration in the vacuum chamber. 3D protein crystals (Zarrine-Afsar *et al.*, 2012) and, very interestingly, membrane protein 2D crystals fixed under ambient conditions on a solid support can be measured using an XFEL, with a flux of 10^{12} photons per pulse (Pedrini *et al.*, 2014 and Frank *et al.*, 2014). Further developments, particularly of high-dynamic range detectors, should make high-resolution routine data collection of 2D crystals feasible, leading, together with improvements in data processing, to radiation-damage-free structures. The use of a solid support (Zarrine-Afsar *et al.*, 2012; Hunter *et al.*, 2014; and Coquelle *et al.*, 2015) instead of a jet could simplify the experimental setup and increase the crystal hit-rate. However, the low scanning speed limited by the grid motion and the selective targeted protein activation in a specific crystal still pose problems and hinder time-resolved structural studies.

SERIAL 3D CRYSTALLOGRAPHY OF MEMBRANE PROTEINS

Serial femtosecond crystallography has been first demonstrated with the membrane protein complex Photosystem I (Shapiro *et al.*, 2008 and Chapman *et al.*, 2011). The need of SFX at a X-FEL for membrane protein structure determination is justified by the fact that membrane proteins have the tendency to grow crystals too small even for microcrystallography at synchrotron sources, with large crystals often being poorly ordered and very difficult to obtain. This emerging method has already enabled the structural determination of several biologically relevant challenging targets like the serotonin 5-HT_{2B} (Liu *et al.*, 2013) and human δ -opioid receptors (Fenalti *et al.*, 2015). It is also noteworthy that the structures of the cytochrome C oxidase (Hirata *et al.*, 2014) and the photosystem II (PSII) complex (Suga *et al.*, 2015) solved at the X-FEL using a standard goniometer-based data collection scheme with larger crystals also show less radiation damage.

FIXED TARGET SERIAL 2D CRYSTALLOGRAPHY OF MEMBRANE PROTEINS

Purified membrane proteins can form 3D- but also 2D crystals (Rigaud *et al.*, 2000 and Abeyrathne *et al.*, 2010). 2D crystals are regular protein arrangements in a lipidic environment providing close-to-physiological structural information, a prerequisite for measuring the protein function. In addition, the readily accessibility of 2D-crystals for diffusing small molecules is an advantage for dynamic studies opening the possibility of using in the future non-light-triggered ligands. X-ray diffraction from individual 2D crystals is not feasible at synchrotron sources, because the sample is damaged well before sufficient Bragg diffraction signal can be detected (Schertler *et al.*, 1993). Like for 3D submicron crystals, X-FELs provide an opportunity to obtain high-resolution diffraction patterns of 2D crystals, whereby the samples have to be

mounted on a flat, transparent membrane which has to be moved after each X-ray pulse to expose a fresh, undamaged area for the subsequent exposure. The first diffraction experiments on native bacteriorhodopsin 2D crystals were performed recently at the Coherent X-Ray Imaging (CXI) experimental station of the Linac Coherent Light Source (LCLS) X-FEL (Frank *et al.*, 2014). The sugar-containing 2D crystal suspension was painted on thin silicon nitride membrane forming the windows of a silicon chip, which was kept in the vacuum of the experimental chamber without cryo-conditions. The sugar prevents the dehydration of 2D crystalline material. A number of diffraction images were recorded by X-ray scanning through the windows, and the observed Bragg peaks provided a proof of principle for the methodology. The diffraction patterns from more recent measurements (Pedrini *et al.*, 2014) acquired after substantial improvement of the beamline demonstrated that the 2D crystals lay flat on the supporting membrane. Indexing of the pattern was easily achieved, and data merging from a dozen single crystal images allowed for unambiguous identification and intensity determination of the diffraction peaks to a resolution of at least 7 Å, significantly improving what could be achieved from single patterns. However, further improvements in resolution are mandatory to reach the length scales for relevant structural and functional considerations. In the short term, potential for improvements lies in modifying sample preparation, reducing the background by optimizing the material of the supporting membrane, improving the X-ray beam by reducing the focus size and increasing the fluence, enhancing the detector performance, and developing dedicated and efficient data acquisition and analysis algorithms *in situ* and *ex situ*, respectively. The latter should also address data sets from non-perpendicular incidence measurements, which will allow one to reconstruct the structure factors necessary for a full 3D electron density map.

Serial fixed target 2D crystallography may develop as a complementary technique to cryo-electron microscopy (cryo-EM), which is rapidly progressing, thanks to detector developments (McMullan *et al.*, 2014). Being a direct imaging technique, cryo-EM measures directly the phases of the structure factors, which markedly facilitates *de novo* structure determination in the static regime. On the other hand, 2D crystallography at X-FELs offers several advantages, most of which are due to the fact that the sample can be kept at room temperature during data acquisition. First, the time consuming optimization of the freezing procedure and cryo-conditions (Goldie *et al.*, 2014) is avoided. Second, pump-probe experiments at near-to-physiological temperatures to explore structural dynamics may become feasible with 2D crystals. Finally, *in situ* control of sample conditions by microfluidic devices appears as an appealing scenario.

X-FEL AND MEMBRANE PROTEIN DYNAMICS

The potential of X-FELs for time-resolved crystallographic studies has recently been demonstrated at the LCLS using the photosystem I-ferredoxin complex (Aquila *et al.*, 2012), the photosystem II complex (Kupitz *et al.*, 2014), and the photoactive yellow protein (Tenboer *et al.*, 2014). By using TR-SFX with an optical pump laser synchronized with the X-FEL, it was possible to obtain X-ray diffraction snapshots from the photoactivated states of proteins. Interestingly, in the absence of crystals, time-resolved wide-angle X-ray scattering (TR-WAXS) on protein in solution showed the potential for free electron lasers to allow the measurement of an ultrafast global conformational change representing a “protein quake” of the photosynthetic system upon multiphoton excitation (Arlund *et al.*, 2014).

Time-delay variations between the pump laser and the probing X-FEL pulse allow for the recording of sequential stages of the protein activation mechanism. By collecting enough X-ray snapshots for each time delay, it will, in principle, be possible to assemble complete molecular movies of protein activation with a temporal resolution from the femtosecond to the millisecond range.

There are several key advantages of TR-SFX compared to more classical approaches to determine the structure of protein intermediate states like cryo-trapping or pump-probe Laue diffraction (Bourgeois and Royant, 2005):

- (1) Proteins inside nano- to micrometer-sized crystals can be more homogeneously activated.
- (2) Dark and excited states are not collected from the same crystal, allowing to investigate

non-reversible systems. (3) The method is less prone to artifacts and provides real-time resolved data in contrast to classical trigger-freeze or freeze-trigger approaches. (4) X-FELs are not restricted to the >100 ps time delay like at synchrotron sources (Schotte *et al.*, 2004). (5) Compared to Laue diffraction methods, TR-SFX can tolerate much higher mosaic spreads of the crystals, common for membrane proteins, and is less dependent on very strongly diffracting crystals. (6) Structural changes are not obscured by radiation damage.

It therefore seems feasible to expand time-resolved crystallographic experiments to the more challenging membrane proteins where very little is known about the structure of reaction intermediates, thus limiting our understanding how they function. So far, TR-SFX depends on a photoactivatable trigger to initiate protein activation. Retinal is such a photochemical switch and acts as a biological cofactor for a number of membrane proteins with diverse functions in prokaryotes to humans. Opsins are retinal-binding proteins belonging to the class of heptahelical transmembrane (7TM) proteins, and understanding the molecular dynamics during activation is of high interest since these proteins not only represent prototypes for the large family of G protein-coupled receptors but are also at the core of many light driven functions in a variety of biological systems. Those include rhodopsin in the perception of light in vision, melanopsin in synchronizing the circadian clocks, bacteriorhodopsin and proteorhodopsins in proton pumping for energy generation, channel rhodopsin in cation transport across biological membranes, and halorhodopsin in osmotic regulation as chloride pump (Ernst *et al.*, 2014). In addition, they are also being used in optogenetics, an important modulation technique in neurobiology, allowing for the spatially and temporally defined activation of nerve cells *in vivo* (Hegemann and Nagel, 2013).

Photochemical isomerization of retinal is one of the fastest reactions in biology, happening within a picosecond in a catalyzing protein environment (Schoenlein *et al.*, 1991). Unfortunately, retinal is prone to radiation damage and doses as low as 0.06 MGy have been reported to lead to structural and spectroscopic alterations (Borshchevskiy *et al.*, 2014). Considering that synchrotron based cryo-crystallography generally exposes crystals to a dose of up to 30 MGy (Garman and Owen, 2006), radiation damage poses a fundamental problem for structural studies of ultrafast retinal reactions with small conformational changes in the Ångström range. Access to femtosecond pulses of modern XFELs will allow us to outrun radiation damage, while obtaining the maximum resolution even for very small crystals in the nanometer range.

TR-SFX AND OPSINS

One well-studied retinal binding 7TM protein is the visual pigment rhodopsin. It belongs to the G protein-coupled receptor family of proteins and was the first retinal binding 7TM protein to be structurally characterized by X-ray crystallography (Palczewski *et al.*, 2000). The apoprotein opsin binds the chromophore 11-cis retinal via a protonated Schiff-base linkage to Lys296. Rhodopsin undergoes conformational changes upon light activation and its intermediate states have been defined spectroscopically (Schertler, 2005). Following the first rhodopsin structure, higher resolution structures of native rhodopsin from bovine retina in the dark state have been reported (Li *et al.*, 2004 and Okada *et al.*, 2004). Freeze-trapping has allowed the structure determination of several rhodopsin intermediates (Nakamichi and Okada, 2006a; 2006b). Opsin extracted from bovine retina yielded structures of both the inactive and the G protein-interacting form (Park *et al.*, 2008; Scheerer *et al.*, 2008; and Park *et al.*, 2013). Soaking opsin crystals with all-trans retinal and the addition of a 11-amino-acid peptide from the C-terminus of G α allowed the determination of the Meta-II structure (Choe *et al.*, 2011). Interestingly, TR-WAXS experiments on rhodopsin in native membrane at the synchrotron (Malmerberg *et al.*, 2015) showed a larger conformational change upon photoactivation than previously suggested by crystallography. Development of a recombinant system for expression and structure determination of rhodopsin mutants (Standfuss *et al.*, 2007) revealed the structure of constitutively active conformations of the receptor (Deupi *et al.*, 2012 and Standfuss *et al.*, 2011) and their relation to human disease (Singhal *et al.*, 2013). Nevertheless, little structural information is

available on earlier rhodopsin intermediates and especially on retinal isomerization in the binding pocket, the very first event in vision, which is decided within only 200 fs. In comparison, the isomerization takes 2–3 ps to complete in solution (Kandori and Maeda, 1995). The quantum yield of the photoisomerization of 11-cis retinal bound to opsin has been experimentally determined to be 0.65 ± 0.01 at 500 nm (Kim *et al.*, 2001; 2003), which is more than twice the quantum yield in solution (Koyama *et al.*, 1991 and Becker, 1988). Retinal protein systems are therefore also excellent models to study catalysis on a heterogeneously structured surface. To date, the only way to structurally analyze this ultrafast and catalytic phenomenon was by using techniques combining high temporal and spectral resolution such as femtosecond-stimulated Raman spectroscopy (Kukura *et al.*, 2005). However, due to the methodological limitations, only a model, lacking the conformational changes of the photoactivation process, can be extrapolated.

TR-SFX on rhodopsin will not only complete the structural dynamic study of known intermediates but also open up the possibility to reveal the very first rearrangements in the retinal binding pocket, which initiate the vision process. Importantly, rhodopsin is one of the two G protein-coupled receptors (GPCRs), the other being the viral US28 (Burg *et al.*, 2015) that can be successfully crystallized as a wild type protein without stabilizing mutations, antibodies or fusion proteins. However, the rhodopsin crystal size and density need to be adapted for the use with a jet sample delivery (Wu *et al.*, 2015). Sub-micron to micron-sized crystals are more suited for time-resolved studies as a more homogenous light activation can be achieved compared with large crystals. The presence of microcrystals can be screened with second harmonic generation (SHG) imaging (Kissick *et al.*, 2011) and powder diffraction provides a fast evaluation the overall crystal quality, which is critical for achieving high enough resolution to visualize subtle changes in the retinal-binding pocket. The ultrafast timescale and the irreversible mechanism of photoactivation of rhodopsin *in vitro* are major challenges. Rhodopsin microcrystals kept in absolute darkness will be sequentially photoactivated with a femtosecond pump laser (480 nm) followed by a highly synchronized probing XFEL pulse at a defined time delay. XFELs represent currently the only possibility to study such ultrafast processes (Fig. 2) with near atomic resolution.

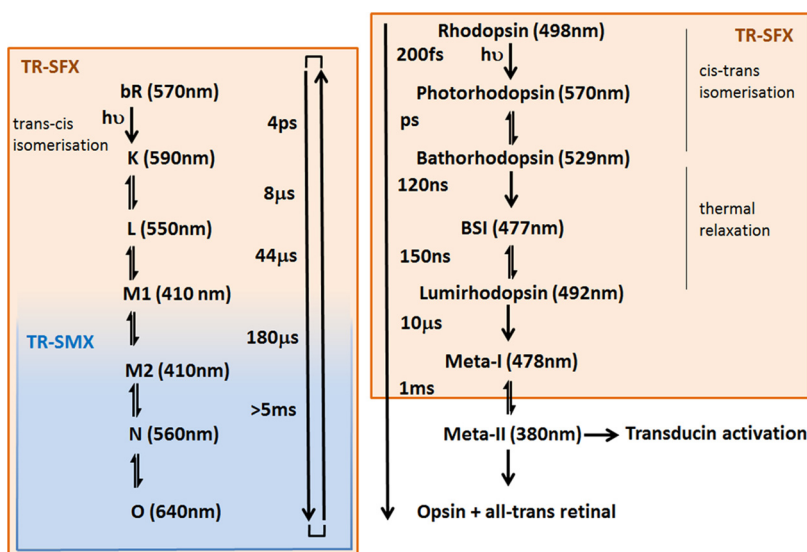


FIG. 2. Time-resolved serial femtosecond crystallography (TR-SFX) studies along the photocycle of the retinal proteins rhodopsin and bacteriorhodopsin (bR). The advent of the X-FEL as a source of very intense X-ray pulses enables to perform now ultrafast time-resolved structural studies at the atomic level. The left panel shows the bacteriorhodopsin photocycle going through the K to O spectral intermediates (Lorenz-Fonfria and Kandori, 2009) and recycling back to the dark state in a few milliseconds. Without a X-FEL (orange box, TR-SFX), the first intermediates could theoretically not be structurally determined, and the later intermediates being in the time-range of synchrotron time-delays (blue box, TR-SMX (time-resolved serial millisecond crystallography)). The right panel shows the photoactivation of rhodopsin (Schertler, 2005) with a first spectral intermediate after already 200 fs.

CONCLUSIONS

The emerging TR-SFX method for the study of structural dynamics is an unique opportunity for the membrane protein field. The recently obtained diffraction studies on 2D membrane protein crystals of bacteriorhodopsin at the X-FEL pave the way for further SFX studies and are of particular interest for the development of TR-SFX. This would allow in the future for time-resolved structural analysis of channels under close-to-physiological conditions. Of general application, the dramatic improvement in the crystal delivery modes as well as in the algorithms for SFX data analysis opens the possibility for a brilliant future for the structural analysis of conformational dynamic studies of photoactivatable proteins, especially from the opsin family. Using caged-compounds for voltage- and ligand-gated neuronal channels (Rullo *et al.*, 2014 and Mourot *et al.*, 2013) would allow for a vast extension of possible target proteins in TR-SFX using either 2D or 3D crystals.

ACKNOWLEDGMENTS

We would like to thank Matthias Frank for leading the FEL experiments on 2D crystals at the X-FEL of the LCLS, Richard Neutze for the support and advices during the X-FEL experiments, and Ilme Schlichting for advices on crystallization. We acknowledge the Swiss Light Source (SLS) crystallization facility and PX beamlines as well as Manfred Burghammer at the esrf (Grenoble, France) and David Sargent (ETH Zürich, Switzerland) for beamtime support and expert advices. SFX experiments on 3D rhodopsin and bR crystals were performed at the LCLS (SLAC, Stanford). We thank the whole consortium for great participation: among them Sebastien Boutet, Garth J. Williams, Dan DePonte, Despina Milathianaki, and Jason E. Koglin from the SLAC, Richard Neutze from the University of Gothenburg, Tom White, Anton Barty, and Henry Chapman from CFEL, and John Spence and Uwe Weierstall from the ASU. *Portions of this research were carried out at the Linac Coherent Light Source (LCLS) at the SLAC National Accelerator Laboratory. LCLS is an Office of Science User Facility operated for the U.S. Department of Energy Office of Science by Stanford University.* The work was financially supported by the grants “co-fund PSI Fellowship” (to P.N.), FP7-PEOPLE-2011-ITN 317079 NanoMem (to W.W.), H2020-MSCA-ITN-2014 637295 X-Probe, the Swiss National Foundation through NCCR MUST (to J.R.), SNF 31003A_141235 (to J.S.), SNF 310030_153145 and 31003A_159558 (to G.S.), the PIER Helmholtz Graduate School and the Helmholtz Association for financial support (to C.G.), and the STC grant, NSF 1231306, respectively.

- Abeyrathne, P. D., Chami, M., Pantelic, R. S., Goldie, K. N., and Stahlberg, H., *Methods Enzymol.* **481**, 25–43 (2010).
Aquila, A. *et al.*, *Opt. Express* **20**, 2706–2716 (2012).
Arlund, D. *et al.*, *Nat. Methods* **11**, 923–926 (2014).
Becker, R. S., *Photochem. Photobiol.* **48**, 369–399 (1988).
Borshchevskiy, V., Round, E., Erofeev, I., Weik, M., Ishchenko, A., Gushchin, I., Mishin, A., Willbold, D., Buldt, G., and Gordeliy, V., *Acta Crystallogr., Sect. D: Biol. Crystallogr.* **70**, 2675–2685 (2014).
Botha, S., Nass, K., Barends, T. R., Kabsch, W., Latz, B., Dworkowski, F., Foucar, L., Panepucci, E., Wang, M., Shoeman, R. L., Schlichting, I., and Doak, R. B., *Acta Crystallogr., Sect. D: Biol. Crystallogr.* **71**, 387–397 (2015).
Bourgeois, D. and Royant, A., *Curr. Opin. Struct. Biol.* **15**, 538–547 (2005).
Boutet, S. *et al.*, *Science* **337**, 362–364 (2012).
Burg, J. S., Ingram, J. R., Venkatakrishnan, A. J., Jude, K. M., Dukupati, A., Feinberg, E. N., Angelini, A., Waghray, D., Dror, R. O., Ploegh, H. L., and Garcia, K. C., *Science* **347**, 1113–1117 (2015).
Chapman, H. N. *et al.*, *Nature* **470**, 73–77 (2011).
Choe, H. W., Park, J. H., Kim, Y. J., and Ernst, O. P., *Neuropharmacology* **60**, 52–57 (2011).
Coquelle, N., Brewster, A. S., Kapp, U., Shilova, A., Weinhausen, B., Burghammer, M., and Colletier, J. P., *Acta Crystallogr., Sect. D: Biol. Crystallogr.* **71**, 1184–1196 (2015).
Deupi, X., Edwards, P., Singhal, A., Nickle, B., Oprian, D., Schertler, G., and Standfuss, J., *Proc. Natl. Acad. Sci. U. S. A.* **109**, 119–124 (2012).
Ernst, O. P., Lodowski, D. T., Elstner, M., Hegemann, P., Brown, L. S., and Kandori, H., *Chem. Rev.* **114**, 126–163 (2014).
Fenalti, G. *et al.*, *Nat. Struct. Mol. Biol.* **22**, 265–268 (2015).
Frank, M. *et al.*, *IUCrJ* **1**, 95–100 (2014).
Garman, E. F. and Owen, R. L., *Acta Crystallogr., Sect. D: Biol. Crystallogr.* **62**, 32–47 (2006).
Goldie, K. N., Abeyrathne, P., Keibel, F., Chami, M., Ringler, P., and Stahlberg, H., *Methods Mol. Biol.* **1117**, 325–341 (2014).
Hegemann, P. and Nagel, G., *EMBO Mol. Med.* **5**, 173–176 (2013).
Hirata, K. *et al.*, *Nat. Methods* **11**, 734–736 (2014).

- Hunter, M. S. *et al.*, *Sci. Rep.* **4**, 6026 (2014).
- Kandori, H. and Maeda, A., *Biochemistry* **34**, 14220–14229 (1995).
- Kim, J. E., Tauber, M. J., and Mathies, R. A., *Biochemistry* **40**, 13774–13778 (2001).
- Kim, J. E., Tauber, M. J., and Mathies, R. A., *Biophys. J.* **84**, 2492–2501 (2003).
- Kissick, D. J., Wanapun, D., and Simpson, G. J., *Annu. Rev. Anal. Chem.* **4**, 419–437 (2011).
- Koyama, Y., Kubo, K., Komori, M., Yasuda, H., and Mukai, Y., *Photochem. Photobiol.* **54**, 433–443 (1991).
- Kukura, P., McCamant, D. W., Yoon, S., Wandschneider, D. B., and Mathies, R. A., *Science* **310**, 1006–1009 (2005).
- Kupitz, C. *et al.*, *Nature* **513**, 261–265 (2014).
- Li, J., Edwards, P. C., Burghammer, M., Villa, C., and Schertler, G. F., *J. Mol. Biol.* **343**, 1409–1438 (2004).
- Liu, W. *et al.*, *Science* **342**, 1521–1524 (2013).
- Lorenz-Fonfria, V. A. and Kandori, H., *J. Am. Chem. Soc.* **131**, 5891–5901 (2009).
- Malmerberg, E., Bovee-Geurts, P. H. M., Katona, G., Deupi, X., Arnlund, D., Wickstrand, C., Johansson, L. C., Westenhoff, S., Nazarenko, E., Schertler, G. F. X., Menzel, A., de Grip, W. J., and Neutze, R., *Sci. Signaling* **8**, ra26 (2015).
- McMullan, G., Faruqi, A. R., Clare, D., and Henderson, R., *Ultramicroscopy* **147**, 156–163 (2014).
- Mourot, A., Tochitsky, I., and Kramer, R. H., *Front. Mol. Neurosci.* **6**, 5 (2013).
- Nakamichi, H. and Okada, T., *Angew. Chem., Int. Ed. Engl.* **45**, 4270–4273 (2006a).
- Nakamichi, H. and Okada, T., *Proc. Natl. Acad. Sci. U. S. A.* **103**, 12729–12734 (2006b).
- Neutze, R., Wouts, R., van der Spoel, D., Weckert, E., and Hajdu, J., *Nature* **406**, 752–757 (2000).
- Nogly, P. *et al.*, *IUCrJ* **2**, 168–176 (2015).
- Okada, T., Sugihara, M., Bondar, A. N., Elstner, M., Entel, P., and Buss, V., *J. Mol. Biol.* **342**, 571–583 (2004).
- Palczewski, K., Kumasaka, T., Hori, T., Behnke, C. A., Motoshima, H., Fox, B. A., Le Trong, I., Teller, D. C., Okada, T., Stenkamp, R. E., Yamamoto, M., and Miyano, M., *Science* **289**, 739–745 (2000).
- Park, J. H., Morizumi, T., Li, Y., Hong, J. E., Pai, E. F., Hofmann, K. P., Choe, H. W., and Ernst, O. P., *Angew. Chem., Int. Ed. Engl.* **52**, 11021–11024 (2013).
- Park, J. H., Scheerer, P., Hofmann, K. P., Choe, H. W., and Ernst, O. P., *Nature* **454**, 183–187 (2008).
- Pedrini, B. *et al.*, *Philos. Trans. R. Soc. London, Ser. B* **369**, 20130500 (2014).
- Perry, S. L., Guha, S., Pawate, A. S., Henning, R., Kosheleva, I., Srajer, V., Kenis, P. J., and Ren, Z., *J. Appl. Crystallogr.* **47**, 1975–1982 (2014).
- Rigaud, J., Chami, M., Lambert, O., Levy, D., and Ranck, J., *Biochim. Biophys. Acta* **1508**, 112–128 (2000).
- Rullo, A., Reiner, A., Reiter, A., Trauner, D., Isacoff, E. Y., and Woolley, G. A., *Chem. Commun.* **50**, 14613–14615 (2014).
- Scheerer, P., Park, J. H., Hildebrand, P. W., Kim, Y. J., Krauss, N., Choe, H. W., Hofmann, K. P., and Ernst, O. P., *Nature* **455**, 497–502 (2008).
- Schertler, G. F., *Curr. Opin. Struct. Biol.* **15**, 408–415 (2005).
- Schertler, G. F., Villa, C., and Henderson, R., *Nature* **362**, 770–772 (1993).
- Schoenlein, R. W., Peteanu, L. A., Mathies, R. A., and Shank, C. V., *Science* **254**, 412–415 (1991).
- Schotte, F., Soman, J., Olson, J. S., Wulff, M., and Anfinrud, P. A., *J. Struct. Biol.* **147**, 235–246 (2004).
- Shapiro, D. A., Chapman, H. N., Deponte, D., Doak, R. B., Fromme, P., Hembree, G., Hunter, M., Marchesini, S., Schmidt, K., Spence, J., Starodub, D., and Weierstall, U., *J. Synchrotron Radiat.* **15**, 593–599 (2008).
- Sierra, R. G. *et al.*, *Acta Crystallogr., Sect. D: Biol. Crystallogr.* **68**, 1584–1587 (2012).
- Singhal, A., Ostermaier, M. K., Vishnivetskiy, S. A., Panneels, V., Homan, K. T., Tesmer, J. J., Vepintsev, D., Deupi, X., Gurevich, V. V., Schertler, G. F., and Standfuss, J., *EMBO Rep.* **14**, 520–526 (2013).
- Standfuss, J., Edwards, P. C., D’Antona, A., Fransen, M., Xie, G., Oprian, D. D., and Schertler, G. F., *Nature* **471**, 656–660 (2011).
- Standfuss, J., Xie, G., Edwards, P. C., Burghammer, M., Oprian, D. D., and Schertler, G. F., *J. Mol. Biol.* **372**, 1179–1188 (2007).
- Suga, M., Akita, F., Hirata, K., Ueno, G., Murakami, H., Nakajima, Y., Shimizu, T., Yamashita, K., Yamamoto, M., Ago, H., and Shen, J. R., *Nature* **517**, 99–103 (2015).
- Sugahara, M. *et al.*, *Nat. Methods* **12**, 61–63 (2015).
- Tenboer, J. *et al.*, *Science* **346**, 1242–1246 (2014).
- Weierstall, U. *et al.*, *Nat. Commun.* **5**, 3309 (2014).
- Weierstall, U., Spence, J. C., and Doak, R. B., *Rev. Sci. Instrum.* **83**, 035108 (2012).
- Wu, W., Nogly, P., Rheinberger, J., Kick, L. M., Gati, C., Nelson, G., Deupi, X., Standfuss, J., Schertler, G., and Panneels, V., “Batch crystallization of rhodopsin for structural dynamics using an X-ray free-electron laser,” *Acta Crystallogr. F Struct. Biol. Commun.* (in press).
- Zarrine-Afsar, A., Barends, T. R., Muller, C., Fuchs, M. R., Lomb, L., Schlichting, I., and Miller, R. J., *Acta Crystallogr., Sect. D: Biol. Crystallogr.* **68**, 321–323 (2012).